0026-895X/11/8004-647–656$25.00
MOLECULAR PHARMACOLOGY
Vol. 80, No. 4
72033/3718212
Mol Pharmacol 80:647–656, 2011
Printed in U.S.A.

Three Arginines in the $GABA_A$ Receptor Binding Pocket Have Distinct Roles in the Formation and Stability of Agonist- versus Antagonist-Bound Complexes

Marcel P. Goldschen-Ohm, David A. Wagner, and Mathew V. Jones

Department of Physiology, University of Wisconsin, Madison, Wisconsin (M.P.G.-O., M.V.J.); and Department of Biological Sciences, Marquette University, Milwaukee, Wisconsin (D.A.W.)

Received March 15, 2011; accepted July 15, 2011

ABSTRACT

Binding of the agonist GABA to the $GABA_A$ receptor causes channel gating, whereas competitive antagonists that bind at the same site do not. The details of ligand binding are not well understood, including which residues interact directly with ligands, maintain the structure of the binding pocket, or transduce the action of binding into opening of the ion channel gate. Recent work suggests that the amine group of the GABA molecule may form a cation-π bond with residues in a highly conserved "aromatic box" within the binding pocket. Although interactions with the carboxyl group of GABA remain unknown, three positively charged arginines (α_1Arg67, α_1Arg132, and β_2Arg207) just outside of the aromatic box are likely candidates. To explore their roles in ligand binding, we individually mutated these arginines to alanine and measured the effects on microscopic ligand binding/unbinding rates and channel gating. The mutations α_1R67A or β_2R207A slowed agonist binding and sped unbinding with little effect on gating, demonstrating that these arginines are critical for both formation and stability of the agonist-bound complex. In addition, α_1R67A sped binding of the antagonist 2-(3-carboxypropyl)-3-amino-6-(4 methoxyphenyl)pyridazinium bromide (SR-95531), indicating that this arginine poses a barrier to formation of the antagonist-bound complex. In contrast, β_2R207A and α_1R132A sped antagonist unbinding, indicating that these arginines stabilize the antagonist-bound state. α_1R132A also conferred a new long-lived open state, indicating that this arginine influences the channel gate. Thus, each of these arginines plays a unique role in determining interactions with agonists versus antagonists and with the channel gate.

Introduction

Activation of the $GABA_A$ receptor involves formation of an agonist-receptor complex (binding) followed by conformational rearrangements that open an integral chloride channel (gating). The ligand binding pocket is formed by the interface between β and α subunits (Sigel et al., 1992; Amin and Weiss, 1993; Smith and Olsen, 1994). Many candidate GABA-binding residues have been identified by observing that their mutation right-shifts the GABA dose-response curve, or that modification of substituted cysteines alters the ability of GABA to activate the channel (Boileau et al., 1999, 2002; Westh-Hansen et al., 1999; Wagner and Czajkowski, 2001; 2002; Newell and Czajkowski, 2003; Holden and Czajkowski, 2002). Recent work has highlighted aromatic residues that are highly conserved among cysteine-loop receptors, including $GABA_A$, nicotinic acetylcholine (nACh), glycine, and 5-hydroxytryptamine$_3$ receptors (Lummis, 2009). Unnatural amino acid substitution of these aromatics demonstrates that the electronegativity of their π-electron orbitals correlates strongly with apparent affinity for agonists, leading to the proposal that the ligand amine group forms a direct cation-π bond with specific aromatic residues. The other end of the GABA molecule, however, is a carboxylate group whose binding partners remain unknown.

The above-mentioned studies used macroscopic measures (e.g., EC_{50}) that are composites of multiple microscopic binding and gating transitions, and thus were not able to distinguish whether a residue is specifically involved in binding, gating, or both. Here, we used submillisecond ligand application and kinetic modeling to estimate the microscopic binding/unbinding rates of agonists and a competitive antagonist.

This work was supported by the the National Institutes of Health National Institute of Neurological Disorders and Stroke [Grant NS046378]; and the American Epilepsy Society and the Lennox Trust Fund.

M.P.G.-O. and D.A.W. contributed equally to this work.

Article, publication date, and citation information can be found at http://molpharm.aspetjournals.org.
doi:10.1124/mol.111.072033.

ABBREVIATIONS: nACh, nicotinic acetylcholine; SR-95531, 2-(3-carboxypropyl)-3-amino-6-(4 methoxyphenyl)pyridazinium bromide (gabazine); THIP, 4,5,6,7-tetrahydroisoxazolo[5,4-c]pyridin-3-ol (gaboxadol); HEK, human embryonic kidney; ANOVA, analysis of variance; P_o, open probability.

By taking advantage of the competition between agonist and antagonist to occupy the agonist binding site, we can determine the agonist binding rate apart from any gating processes (Clements et al., 1992; Jones et al., 1998, 2001; Wagner et al., 2004).

The substituted cysteine accessibility method (Boileau et al., 1999; Wagner and Czajkowski, 2001) and homology modeling (Cromer et al., 2002) have identified three arginines (α_1Arg67, α_1Arg132, and β_2Arg207) at the β/α intersubunit ligand-binding interface, in positions in which they could serve as binding partners for the carboxylate group of GABA (Fig. 1A). We showed previously that in the rat $\alpha_1\beta_2$ $GABA_A$ receptor, mutating β_2Arg207 to cysteine slowed GABA binding and sped unbinding, with no effect on gating (Wagner et al., 2004), raising the possibility that β_2Arg207 could directly interact with GABA. Here, we compare the roles of all three arginines in the human receptor by mutating them individually to alanine, which more closely approximates the removal of the native side chain than mutation to cysteine.

We find that α_1Arg67 and β_2Arg207 are critical for both rapid and stable binding of the agonists GABA and THIP but not for channel gating. In contrast, α_1Arg67 hinders binding of the competitive antagonist 2-(3-carboxypropyl)-3-amino-6-(4-methoxyphenyl)pyridazinium bromide (SR-95531), whereas β_2Arg207 and α_1Arg132 stabilize bound antagonist. Mutation of α_1Arg132 also confers a new open state. Thus, α_1Arg67 and β_2Arg207 are good candidates for interacting directly with GABA, whereas β_2Arg207 and α_1Arg132 may interact with antagonist and α_1Arg132 may also participate in transducing binding to gating.

Materials and Methods

Cell Culture and Transfection. Human embryonic kidney (HEK-293) cells were cultured in minimum essential medium with Earle's salts (Mediatech, Inc., Herndon, VA) containing 10% bovine calf serum (Sigma-Aldrich, St. Louis, MO) in a 37°C incubator under a 5% CO_2 atmosphere. Cells were transfected using either a calcium phosphate precipitation method (Jordan et al., 1996) or with the Lipofectamine 2000 reagent (Invitrogen, Carlsbad, CA) with the prescribed protocol, with 1 to 2 μg total of one α and one β construct in a 1:1 ratio, from α_1, α_1R67A, or α_1R132A and β_2, $\beta_{2\text{-GKER}}$ (see below), or β_2R207A human cDNAs in vector pcDNA3.1 (Invitrogen). Recordings were performed 24 to 80 h after transfection. Wild-type constructs were obtained from Dr. Steven Petrou (Howard Florey Institute, Melbourne, Australia), and mutant constructs were made using recombinant polymerase chain reaction as described previously (Kucken et al., 2000). Each mutation was verified by double-stranded sequencing of the entire coding region to verify that no unwanted mutations had been introduced during the procedure.

Patch-Clamp Electrophysiology. Recordings from outside-out patches excised from HEK-293 cells were made using borosilicate glass pipettes filled with 140 mM KCl, 10 mM EGTA, 2 mM MgATP, 20 mM phosphocreatine, and 10 mM HEPES, pH 7.3, with osmolarity of 315 mOsM. Patches were voltage-clamped at −60 mV and placed in the stream of a multibarreled flow-pipe array (Vitrodynamics, Rockaway, NJ) mounted on a piezoelectric bimorph (Morgan Electro Ceramics Inc., Bedford, OH). A computer-controlled constant current source drove the bimorph to move solution interfaces over the patch with 10 to 90% exchange times of <200 μs, as measured by the liquid junction current at the open pipette tip after each experiment. Junction currents were generated by altering the ionic strength with an additional 5 mM NaCl or 1% H_2O in solutions containing agonist or antagonist, respectively. GABA, THIP, and SR-95531 were dissolved in the perfusion solution, which usually contained 145 mM NaCl, 2.5 mM KCl, 2 mM $CaCl_2$, 1 mM $MgCl_2$, 10 mM HEPES, and 4 mM glucose, pH 7.4, with osmolarity of 320 mOsM adjusted with sucrose. For extracellular solutions that contained greater than 30 mM GABA or THIP, the concentration of NaCl was reduced, and the appropriate combination of sucrose and

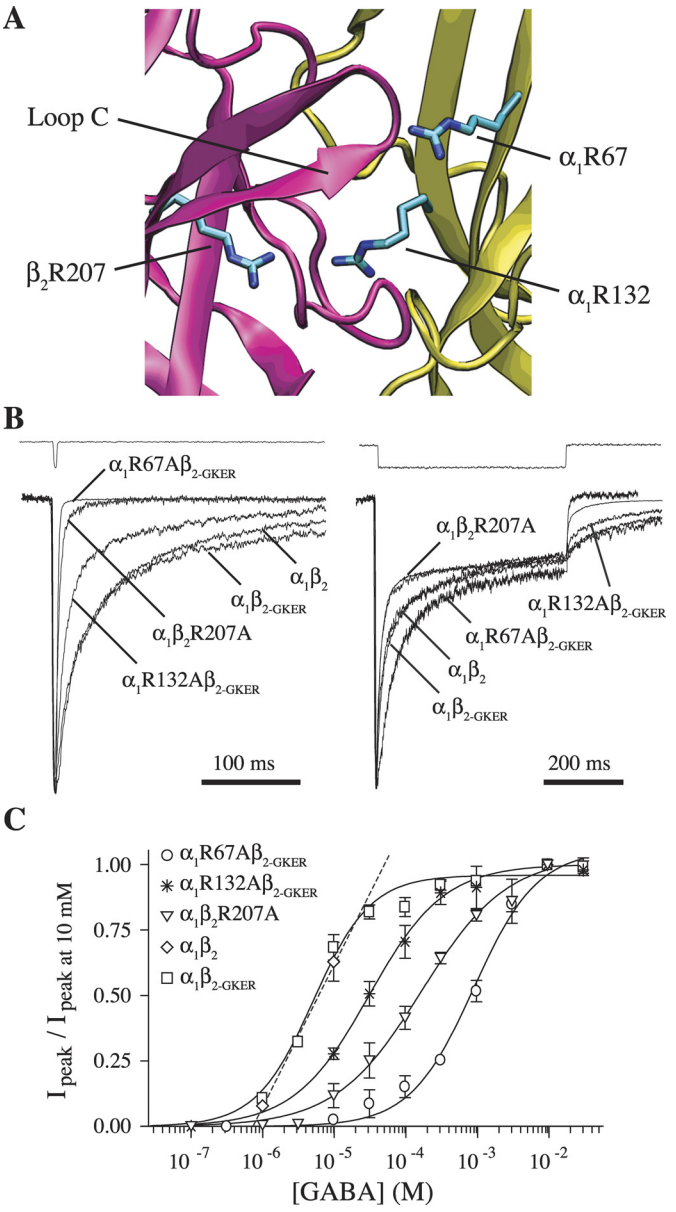

Fig. 1. Mutation of β_2Arg207, α_1Arg67, or α_1Arg132 to alanine increases the rate of deactivation and right-shifts concentration-response curves but does not affect desensitization. A, homology model of the $GABA_A$ receptor agonist binding site at the interface between β_2 (pink) and α_1 (yellow) subunits showing residues β_2Arg207, α_1Arg67, and α_1Arg132 (O'Mara et al., 2005; with α_1Arg67 rotated arbitrarily so as to protrude into the binding pocket). B, mutants and wild-type receptors were challenged with 2 to 4 ms (left) or 500 ms (right) pulses of 10 mM GABA (because of differences in EC_{50}, we ensured saturation by using 30 mM GABA for R67A). All traces were normalized to their peak to ease comparison. Peak currents of traces shown varied between 60 and 300 pA. Each trace is the average of between 8 and 25 sweeps, recorded while the patches were held at −60 mV. The top traces in both are example recordings from open pipette tips at the end of an experiment to demonstrate solution exchange. C, GABA concentration-response curves of peak currents, fit with the equation $I_{GABA}/I_{GABA\text{-}max} = Y_{max}/[(EC_{50}/[GABA])^N + 1]$, where N is the Hill coefficient (Prism 4). Only two data points are shown for $\alpha_1\beta_2$, which were linearly interpolated to estimate EC_{50} (Table 2).

agonist was added to compensate for the reduced osmolarity. When using low NaCl extracellular solution, the concentration of KCl in the pipette solution was also reduced to maintain a constant Cl^- driving force, and potassium gluconate was added to maintain the osmolarity. All chemicals were obtained from Sigma-Aldrich. Currents were low-pass-filtered at 2 to 5 kHz with a four-pole Bessel filter and digitized at a rate no less than twice the filter frequency. Data were collected using an Axopatch 200B amplifier and Digidata 1320A digitizer (Molecular Devices, Sunnyvale, CA), controlled by AxoGraph software (Axograph Scientific, Sydney, Australia) running on a Macintosh G4 (Apple Computer, Cupertino, CA). Curve-fitting was performed using either AxoGraph or Prism 4 (GraphPad Software, Inc., San Diego, CA) software. Deconvolution of antagonist unbinding experiments (Jones et al., 2001) was done using home-written routines in MATLAB 7 (The MathWorks, Natick, MA).

Statistical Analysis. In all cases, significant differences were tested using one-way ANOVA with post hoc Tukey test at a significance level of $p < 0.05$ (Prism 4). Weighted time constants (τ_w) for biexponential fits to macroscopic kinetics [i.e., $I(t) = \Sigma_i a_i \exp(-t/\tau_i)$] were calculated as $\tau_w = \Sigma_i a_i \tau_i$, where a_i and τ_i are the fractional amplitude and time constant of the i^{th} component, I is current, and t is time.

β_2-Subunit GKER Mutation. The $GABA_A$ receptor mutation α_1R67A (human numbering, equivalent to Arg66 in the rat) has been shown previously to disrupt receptor assembly with the β_2 subunit (Bollan et al., 2003). Consistent with these findings, we observed very little GABA-evoked current in outside-out patches from HEK-293 cells transfected with α_1R67A and β_2 subunits (3 of 50 patches had detectable current with a mean of 8 pA). However, it has also been reported that assembly in the presence of α_1R67A can be rescued by replacing four amino acid residues in the β_2 subunit with the aligned residues from the β_3 subunit (Taylor et al., 1999; Bollan et al., 2003). We refer to this construct as $\beta_{2\text{-GKER}}$ representing the four mutations D171G, N173K, T179E, and K180R.

Single-Channel Records. Single-channel currents were recorded in the presence of 30 mM GABA from patches held at −80 mV, sampled at 20 kHz, and filtered at 2 kHz. Openings and closures were defined by entry into specific amplitude windows using a 200-μs minimum event width, with home-written routines in MATLAB 7 (The MathWorks). Events that included multiple openings were discarded. Open time distributions were fitted by the maximum likelihood method, with corrections for missed events (Colquhoun and Sigworth, 1995).

Nonstationary Variance Analysis. Nonstationary variance analysis (Sigworth, 1980) was performed on responses to repeated pulses of saturating GABA (10 mM), from which ensemble mean current (I) and variance (σ^2) were calculated at each time point. The mean current was divided into 100 equally sized bins, and the variances in each bin were averaged. Plots of binned variance versus current were fit with the equation $\sigma^2 = iI - I^2N^{-1}$, where i is the single channel current and N is the number of channels. Conductance was computed by dividing i by the holding potential of −60 mV. Variance resulting from slow drift (i.e., rundown or run-up) was corrected by local linear fitting of the drift, calculating the variance due to this trend at each point, and subtracting this drift variance (scaled by the square of normalized current amplitude) from the total variance before fitting. This method yields accurate estimates of i and N when tested on simulated data with drift.

Kinetic Modeling. Kinetic modeling was performed with home-written software using the Q-matrix method (Colquhoun and Hawkes, 1995). Before optimization of the model shown in Fig. 7A, the GABA binding rate constant k_{on} was fixed to the value we determined experimentally (Table 2), and the maximal open probability ($P_{o\text{-max}}$) was set to 0.44 based on nonstationary variance analysis (Fig. 6). The remaining unconstrained rate constants were optimized for individual patches expressing $\alpha_1\beta_2$, $\alpha_1\beta_2$R207A, or α_1R67A$\beta_{2\text{-GKER}}$ receptors by fitting current responses to 2 to 4 ms and 500-ms pulses of 10 to 30 mM GABA (Fig. 7, B and C). Optimization used a Nelder-Mead simplex algorithm to minimize the amplitude-weighted sum of squared errors between actual and simulated currents. In all cases, significant differences in fitted parameters between constructs were tested using one-way ANOVA with post hoc Tukey's test, $p < 0.05$.

Results

Arginines α_1Arg67, α_1Arg132, and β_2Arg207 Are Critical for Prolonged Receptor Activation. Responses to rapid ligand application were recorded in outside-out patches from HEK-293 cells transfected with either $\alpha_1\beta_2$, $\alpha_1\beta_2$R207A, $\alpha_1\beta_{2\text{-GKER}}$, α_1R67A$\beta_{2\text{-GKER}}$, or α_1R132A$\beta_{2\text{-GKER}}$ subunit combinations. Receptor kinetics were characterized by macroscopic deactivation after brief pulses (2–4 ms), somewhat similar to that occurring during synaptic transmission, and desensitization during long pulses (500 ms) of saturating GABA (10–30 mM). The β_2 subunit GKER mutation was employed to rescue receptor assembly in the presence of α_1R67A or α_1R132A (see *Materials and Methods*). Compared with $\alpha_1\beta_2$ receptors, $\alpha_1\beta_{2\text{-GKER}}$ did not alter macroscopic deactivation or desensitization kinetics, or GABA EC_{50} (Fig. 1, B and C; Table 1). Thus, we treated $\alpha_1\beta_{2\text{-GKER}}$ as a "wild-

TABLE 1

Summary of biexponential fits to deactivation and desensitization

Arginine-to-alanine mutations α_1R67A, α_1R132A, and β_2R207A sped deactivation after brief (2–4 ms) pulses of 10 to 30 mM GABA, with little effect on desensitization during longer (500-ms) pulses. Data are mean ± S.E.M. "Remaining" indicates fraction of peak current remaining at the end of a 500-ms pulse.

	τ_{fast}	τ_{fast}	τ_{slow}	τ_{slow}	$\tau_{weighted}$	Remaining	n
	ms	%	*ms*	%	*ms*	%	
Deactivation after brief GABA pulses (2–4 ms, 10 mM)							
$\alpha_1\beta_2$	26 ± 2	72 ± 5	298 ± 18	29 ± 5	103 ± 14	N.A.	9
$\alpha_1\beta_{2\text{-GKER}}$	22 ± 3	71 ± 3	281 ± 31	29 ± 3	96 ± 12	N.A.	9
$\alpha_1\beta_2$R207A	6 ± 1*	90 ± 5*	31 ± 5*	10 ± 5*	8 ± 1*	N.A.	4
α_1R67A$\beta_{2\text{-GKER}}$	4 ± 1*	98 ± 2*	15 ± 3*	2 ± 2*	4 ± 1*	N.A.	7
α_1R132A$\beta_{2\text{-GKER}}$	13 ± 2*	81 ± 1	161 ± 31*	19 ± 1	42 ± 8*	N.A.	4
Desensitization during long GABA pulses (500 ms, 10 mM)							
$\alpha_1\beta_2$	13 ± 1	50 ± 3	159 ± 14	20 ± 2	57 ± 10	27 ± 2	32
$\alpha_1\beta_{2\text{-GKER}}$	18 ± 1	49 ± 1	239 ± 30	23 ± 2	88 ± 11	28 ± 2	25
$\alpha_1\beta_2$R207A	11 ± 1	62 ± 3	184 ± 18	15 ± 2	42 ± 5	23 ± 2	39
α_1R67A$\beta_{2\text{-GKER}}$[a]	27 ± 3*	37 ± 4	217 ± 26	27 ± 3	107 ± 13	36 ± 3	15
α_1R132A$\beta_{2\text{-GKER}}$	11 ± 1	62 ± 3	267 ± 61	17 ± 2	70 ± 15	21 ± 2	16

N.A., not available.

[a] Currents were elicited with 30 mM GABA.

* Differences between mutants and their appropriate control (see *Results*) were calculated using one-way ANOVA with post-hoc Tukey test at $p < 0.05$ (Prism 4).

type" control for the α_1R67A and α_1R132A mutants, whereas the β_2R207A mutant was compared with $\alpha_1\beta_2$.

All three mutations accelerated deactivation (speeding of τ_w: α_1R67A, 24-fold; α_1R132A, 2-fold; β_2R207A, 13-fold), with little or no effect on desensitization (Fig. 1B, Table 1). Although α_1R67A exhibited a slower initial component of desensitization, it sped deactivation to a much larger degree than it slowed desensitization. Both macroscopic deactivation and desensitization emerge from the interactions of numerous microscopic transitions. However, only deactivation depends on ligand unbinding, because in the presence of saturating ligand, any unbound receptor will immediately rebind (it is "as if" the ligand never unbinds). Speeding deactivation without appreciably altering desensitization therefore suggests that all three mutations increase the unbinding rate of GABA, with little or no effect on gating (further evidence for this conclusion for α_1R67A and β_2R207A is presented below). Faster unbinding should reduce the time spent in ligand-bound states, which predicts a lower apparent affinity. Consistent with this interpretation, all three mutations shifted the GABA dose-response curve to the right (shift in GABA EC_{50}: α_1R67A, 183-fold; α_1R132A, 5-fold; β_2R207A, 23-fold) (Fig. 1C, Table 2).

Arginines Are Differentially Involved in Competitive Antagonist Binding. Competitive antagonists are likely to bind at the same location as GABA, thus preventing GABA from binding, but there must be a difference in the way they interact with the binding site because they do not induce channel opening. We therefore asked whether α_1Arg67, α_1Arg132, or β_2Arg207 were involved in binding the competitive antagonist SR-95531 by examining the effect of their individual alanine mutations on SR-95531 microscopic binding and unbinding rates.

The unbinding rate of a competitive antagonist can be obtained from macroscopic currents using a deconvolution based method described in detail by Jones et al. (2001). In brief, receptors are pre-equilibrated in antagonist and then rapidly switched to a solution with saturating GABA alone. The resulting current is due to antagonist unbinding from receptors that are then free to bind GABA and open (Fig. 2A). This current is the convolution of the antagonist unbinding time course with the response to GABA alone. Therefore, the antagonist unbinding time course can be obtained by deconvolving the currents after antagonist equilibration with a control response to saturating GABA (Fig. 2B). In our hands, the unbinding time course of SR-95531 from the $GABA_A$ receptor obtained by this and other methods (e.g., Jones et al., 1998) has always been monoexponential, suggesting unbinding from a single site. Thus, we take the inverse of this time constant to be the microscopic antagonist unbinding rate (Table 2).

In addition to the unbinding rate, the amount of current elicited immediately upon agonist application reflects the equilibrium fraction of receptors having bound antagonist during the pre-equilibration, which depends on the antagonist concentration. All three mutants altered the affinity of the receptor for SR-95531, as evidenced by their shifted inhibition dose-response curves, but not in the same direction (Fig. 2C, Table 2). Consistent with the monoexponential nature of SR-95531's unbinding time course (Fig. 2B), the inhibition dose-response curves for each construct were best fitted with a Hill slope near unity (Fig. 2C, inset), suggesting that antagonism occurs upon binding of a single molecule of SR-95531. For a single binding site, as seems to be the case for SR-95531 (see *Discussion*), the antagonist binding rate can be computed as $k_{on\text{-}ant} = k_{off\text{-}ant}/K_D$, where the microscopic dissociation constant K_D is the antagonist concentration required to block half of the channels.

The lower antagonist affinities conferred by β_2R207A and α_1R132A were entirely due to a 2- and 9-fold increase in the SR-95531 unbinding rate, respectively (Table 2). On the other hand, the higher affinity conferred by α_1R67A was due to a 5-fold increase in the SR-95531 binding rate. This indicates that α_1Arg67 acts as a barrier to binding SR-95531, whereas α_1Arg132 and to a lesser extent β_2Arg207 stabilize the SR-95531-bound complex.

Arginines α_1Arg67 and β_2Arg207 Are Required for Fast Agonist Binding. To determine the roles of α_1Arg67, α_1Arg132, and β_2Arg207 in GABA binding, we examined the effect of their individual alanine mutations on the microscopic GABA binding rate using a macroscopic measure that involves "racing" GABA against the competitive-antagonist SR-95531. In brief, control responses to saturating GABA were interleaved with responses to the simultaneous application of GABA and SR-95531. Coapplication of agonist and antagonist leads to a reduction in the peak agonist-evoked response as a result of some of the receptors binding antagonist and contributing no current. The ratio I_{race} of the peak current in the presence of antagonist to that in control depends on the relative concentrations and binding rates of the agonist and antagonist as they "race" against each other for the binding site. If the antagonist binding rate ($k_{on\text{-}ant}$) is known, the agonist binding rate can be computed as $k_{on\text{-}ag} = [ant]\ k_{on\text{-}ant}/([ag](1/I_{race} - 1))$, where $[ant]$ and $[ag]$ are the antagonist and agonist concentrations, respectively (Jones et al., 1998).

TABLE 2

Summary of microscopic binding/unbinding rates and affinities for the competitive antagonist SR-95531 and binding rates and macroscopic affinities for the agonists GABA and THIP

Data are mean ± S.E.M.

	$K_{D\text{-}SR}$	$k_{off\text{-}SR}$	$k_{on\text{-}SR}$	$EC_{50\text{-}GABA}$	$k_{on\text{-}GABA}$	$k_{on\text{-}THIP}$
	nM	s^{-1}	$M^{-1}{\cdot}s^{-1}$	*mM*	$M^{-1}{\cdot}s^{-1}$	
$\alpha_1\beta_2$	124	10 ± 1	$(8.2 \pm 0.7) \times 10^7$	6	$(2.2 \pm 0.4) \times 10^7$	$(5.5 \pm 0.7) \times 10^6$
$\alpha_1\beta_{2\text{-GKER}}$	69	7 ± 1	$(9.7 \pm 0.8) \times 10^7$	8	$(2.0 \pm 0.2) \times 10^7$	N.A.
$\alpha_1\beta_2$R207A	230	23 ± 2*	$(9.9 \pm 1.0) \times 10^7$	139	$(3.8 \pm 0.4) \times 10^{6}$*	$(1.9 \pm 0.7) \times 10^{5}$*
α_1R67A$\beta_{2\text{-GKER}}$	26	12 ± 2	$(4.5 \pm 0.6) \times 10^{8}$**	1100	$(1.4 \pm 0.1) \times 10^{6}$*	$(5.6 \pm 1.7) \times 10^{5}$*
α_1R132A$\beta_{2\text{-GKER}}$	542	63 ± 9*	$(1.2 \pm 0.2) \times 10^8$	31	$(1.7 \pm 0.4) \times 10^7$	N.A.

N.A., not available.

* Differences between mutants and their appropriate control (see *Results*) were calculated using one-way ANOVA with post-hoc Tukey test at $p < 0.05$ (Prism 4). GABA unbinding rates were also estimated using a kinetic model (see Fig. 7).

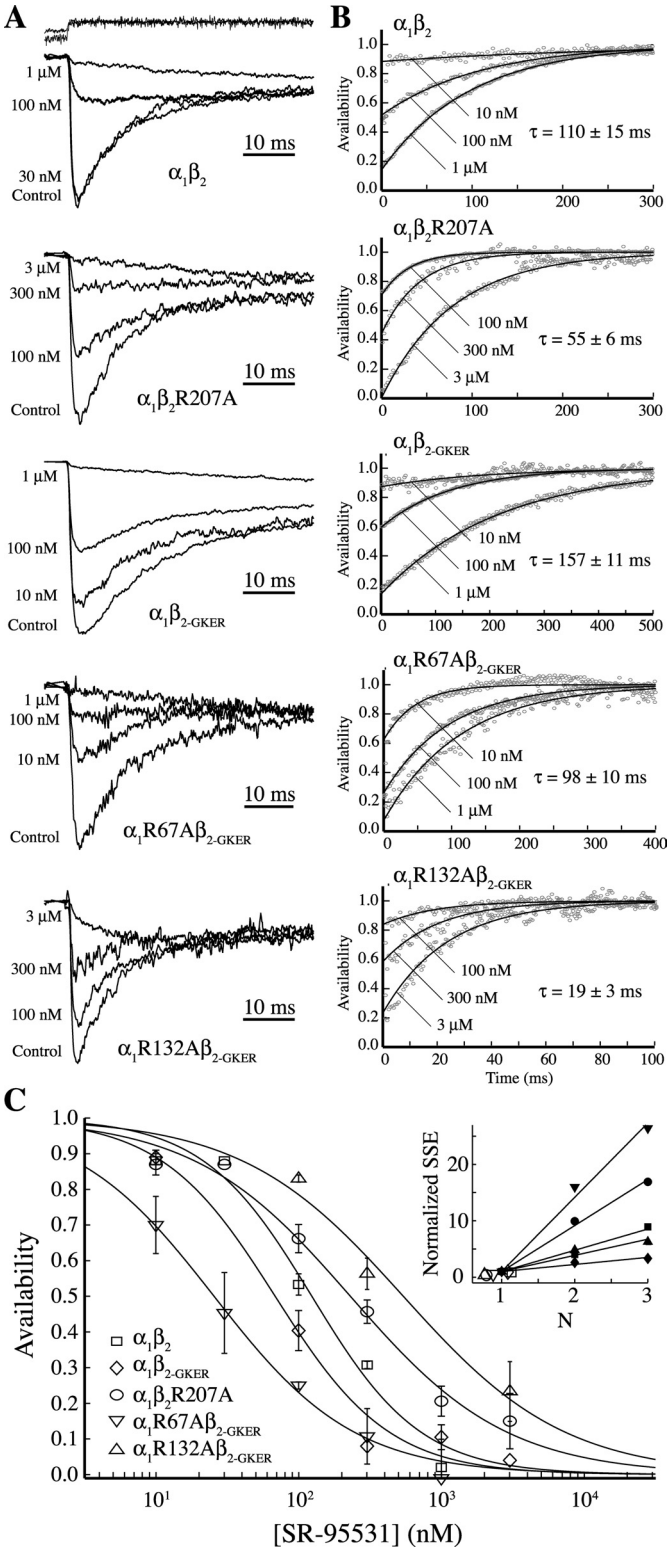

Fig. 2. Unbinding kinetics and affinity of the competitive antagonist SR-95531. A, currents evoked with 10 to 30 mM GABA both without (control) and with pre-equilibration in the competitive antagonist SR-95531 (concentrations given to the left of each trace). B, the antagonist unbinding time course was obtained by deconvolving the control (no antagonist pre-equilibration) currents and the currents after equilibration in antagonist. Deconvolutions (gray circles) were fit to the equation $A(t) = [P_\infty - (P_\infty - P_0)\exp(-t/\tau)]^N$, where $A(t)$ is the fraction of available receptors (antagonist not bound at any site), P_0 and P_∞ are the probabilities that a single binding site is available initially at $t = 0$ and at steady state as $t \to \infty$, τ is the time constant of antagonist unbinding from each site ($k_{\text{off-SR}} = 1/\tau$), and N is the number of antagonist binding sites (Jones et al., 2001). Best fits were always obtained with $N = 1$. Note the different time scales for each construct. C, dose-response curves for the equilibrium antagonist occupancy in the absence of GABA, $A(t = 0)$, were fitted to the normalized Hill equation $I/I_{\max} = 1 - 1/[(K_{\text{D-SR}}/[\text{SR} - 95531])^N + 1]$. Unconstrained fits (shown) had Hill coefficients (N) near unity for all five constructs ($\alpha_1\beta_2$, 1.1; R207A, 0.8; $\alpha_1\beta_{2\text{-GKER}}$, 1.1; R67A, 0.9; R132A, 0.8). The goodness of fit as judged by the sum-of-squared errors (SSE) decreased for increasing integer N (inset, SSE normalized to value at $N = 1$; solid symbols, N constrained to integers 1, 2, or 3; open symbols, N unconstrained).

In wild-type receptors, simultaneous application of 10 mM GABA and 300 μM SR-95531 blocked ~15% of the peak current obtained by application of GABA alone (Fig. 3). This suggests that SR-95531 "out-raced" GABA for its binding site at 15% of the receptors. In contrast, peak current for the β_2R207A mutant was blocked by ~45% under the same conditions. Because this mutation does not affect the binding rate of SR-95531, it must be that β_2R207A slows GABA binding. Peak current for the α_1R67A$\beta_{2\text{-GKER}}$ mutant was 10-fold more sensitive to SR-95531 than that for β_2R207A. However, part of this enhanced sensitivity is due to the faster binding rate of SR-95531, which when taken into account yields a 14- and 6-fold slowing of the GABA binding rate compared with wild type for the α_1R67A and β_2R207A mutants, respectively. In contrast, α_1R132A did not confer a detectable difference in the GABA binding rate. Therefore, α_1Arg67 and β_2Arg207, but not α_1Arg132, are required for rapid formation of the GABA-bound complex.

To test whether α_1Arg67 and β_2Arg207 are specifically involved only in binding GABA, or if they are more generally involved in agonist binding, we examined the effect of their mutation to alanine on the microscopic binding rate of the lower affinity agonist THIP. Similar to their effect on GABA binding, both α_1R67A and β_2R207A slowed THIP binding, suggesting that these residues may play a generic role in agonist binding at the $GABA_A$ receptor (Fig. 4, Table 2).

Mutations α_1R67A and β_2R207A Do Not Alter Peak Open Probability, Open Time, or Conductance. Because none of the mutations had much of an effect on macroscopic desensitization, we hypothesized that they did not greatly affect gating. To test this, we examined the effect of each mutation on multiple aspects of channel gating including single-channel conductance, open dwell time distributions, and maximal open probability ($P_{\text{o-max}}$). Open dwell time distributions from single-channel recordings in the presence of 30 mM GABA at a holding potential of −80 mV for $\alpha_1\beta_2$, α_1R67A$\beta_{2\text{-GKER}}$, and $\alpha_1\beta_2$R207A were all fitted with three exponential components whose time constants and relative areas were not different (Fig. 5). Although the first three time constants of the open dwell time distribution for α_1R132A$\beta_{2\text{-GKER}}$ were also similar to wild type, we observed a small fraction of longer openings not seen in the other constructs. Mean open times (and relative areas) were the following: for $\alpha_1\beta_2$ (eight patches, mean ± S.E.M.), 0.3 ± 0.03 ms (0.57 ± 0.05), 1.0 ± 0.1 ms (0.39 ± 0.05), and 4.2 ± 0.4 ms (0.05 ± 0.01); α_1R67A$\beta_{2\text{-GKER}}$ (four patches), 0.3 ± 0.1 ms (0.64 ± 0.06), 0.9 ± 0.2 ms (0.34 ± 0.05), and 3.0 ± 0.4 ms (0.03 ± 0.01); α_1R132A$\beta_{2\text{-GKER}}$ (three patches), 0.4 ± 0.04 ms (0.42 ± 0.01), 1.1 ± 0.2 ms (0.43 ± 0.01), 3.9 ± 1.1 ms (0.14 ± 0.01), and 16.1 ± 3.2 ms (0.01 ± 0.003); and $\alpha_1\beta_2$R207A (four patches), 0.2 ± 0.02 ms (0.56 ± 0.03), 0.7 ± 0.1 ms (0.42 ± 0.03), and 3.1 ± 0.4 ms (0.02 ± 0.01). In addition, none of the mutations

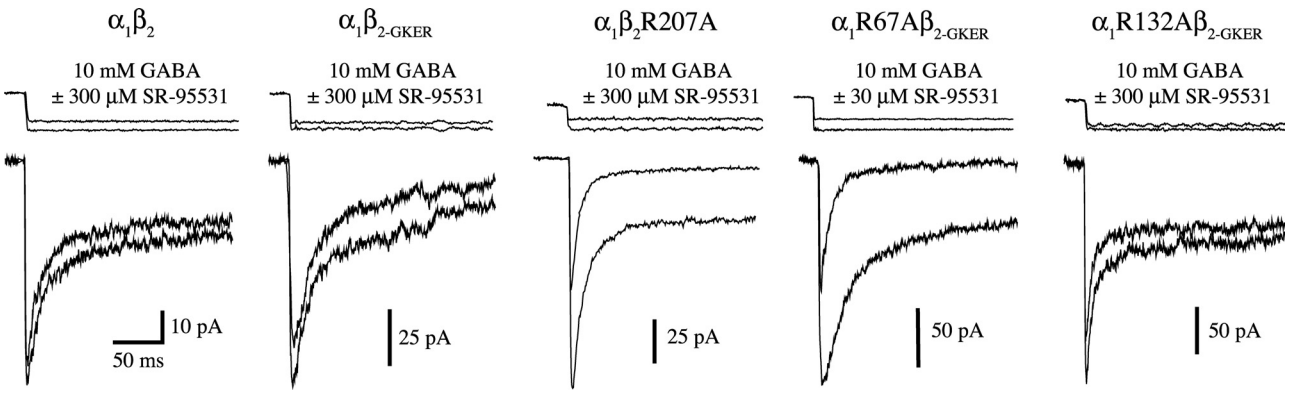

Fig. 3. The mutations β_2R207A and α_1R67A slow the GABA binding rate. Responses to simultaneous application of GABA and the competitive antagonist SR-95531 reflect their relative binding rates. The larger amplitude traces are responses to GABA alone, whereas the smaller traces are responses to coapplication of GABA and antagonist. The ratio of the peak currents was used to compute $k_{\text{on-GABA}}$ (Jones et al., 1998). Each trace is the average of between 5 and 20 sweeps. The top traces are recordings from open pipette tips made at the end of each experiment.

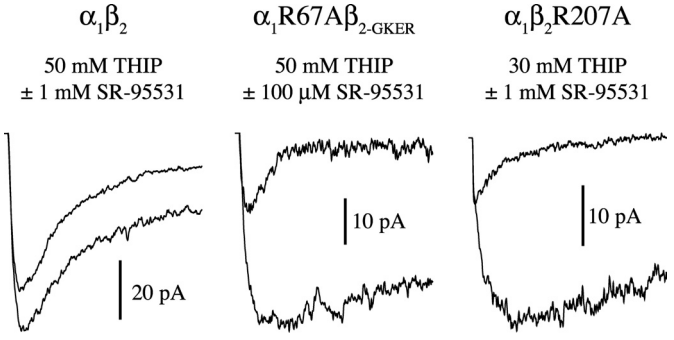

Fig. 4. The mutations β_2R207A and α_1R67A slow the binding rate of THIP. Responses to simultaneous application of THIP and the competitive antagonist SR-95531 reflect their relative binding rates. Pulses were 500 ms and the first 100 ms are shown. The larger amplitude traces are responses to THIP alone, whereas the smaller traces are responses to coapplication of THIP and antagonist. The ratio of the peak currents was used to compute $k_{\text{on-THIP}}$ (Jones et al., 1998).

altered the channel's main conductance level, which was the following: for $\alpha_1\beta_2$ (mean ± S.E.M.), 10.7 ± 0.6 pS; R67A$\beta_{2\text{-GKER}}$, 9.3 ± 0.3 pS; R132A$\beta_{2\text{-GKER}}$, 8.6 ± 0.4 pS; and $\alpha_1\beta_2$R207A, 9.9 ± 0.8 pS. Differences were assessed by one-way ANOVA with post hoc Tukey's test at $p < 0.05$.

Closed dwell time distributions were fit with four exponential components (data not shown). Mean closed times (and relative areas) for $\alpha_1\beta_2$ were 0.9 ± 0.1 ms (0.53 ± 0.04), 7.4 ± 0.8 ms (0.28 ± 0.04), 183 ± 52 ms (0.14 ± 0.05), and 1856 ± 686 ms (0.04 ± 0.01). None of the mutants differed in any of these components. However, because patches probably contained multiple channels, the observed closed times include apparent closures that may be due to the closing of one channel and the opening of another. Because these apparent closures are less likely to occur during sojourns to short-lived closed states, we examined closed time distributions from within bursts of openings separated by closures longer than 10 ms, excluding those bursts containing stacked openings. Within-burst closed-time distributions were fit with three exponential components. Mean within burst closed times (and relative areas) for $\alpha_1\beta_2$ were 0.3 ± 0.04 (0.26 ± 0.05), 1.5 ± 0.2 (0.45 ± 0.03), and 8.7 ± 0.6 ms (0.30 ± 0.04). None of the mutants differed in any of these components.

We used nonstationary variance analysis (Sigworth, 1980) to estimate both the single-channel conductance and $P_{\text{o-max}}$

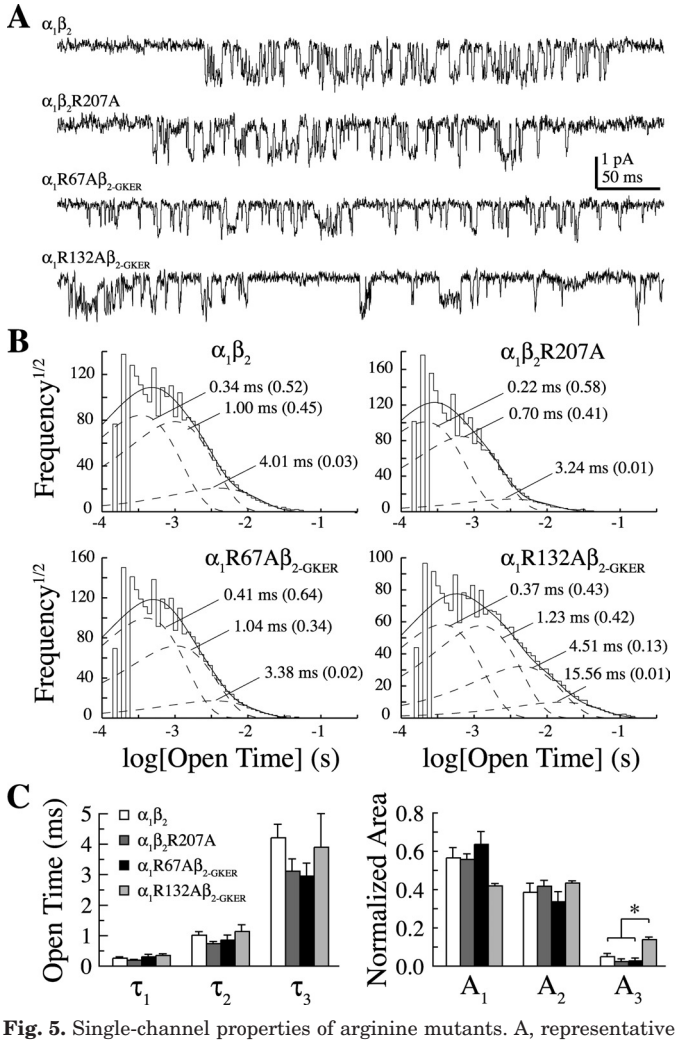

Fig. 5. Single-channel properties of arginine mutants. A, representative single channel events. Recordings were filtered at 2 kHz for analysis and 1 kHz for display. B, open dwell time distributions across patches were fit with the sum of three to four exponentials (time constants and relative areas are labeled). The first three time constants were not different in the mutants, but α1R132A receptors exhibited a small number of additional long-lived openings not seen for the other three constructs. C, summary of the first three open dwell time constants and relative areas. *, different by one-way ANOVA with post hoc Tukey's test at $p < 0.05$.

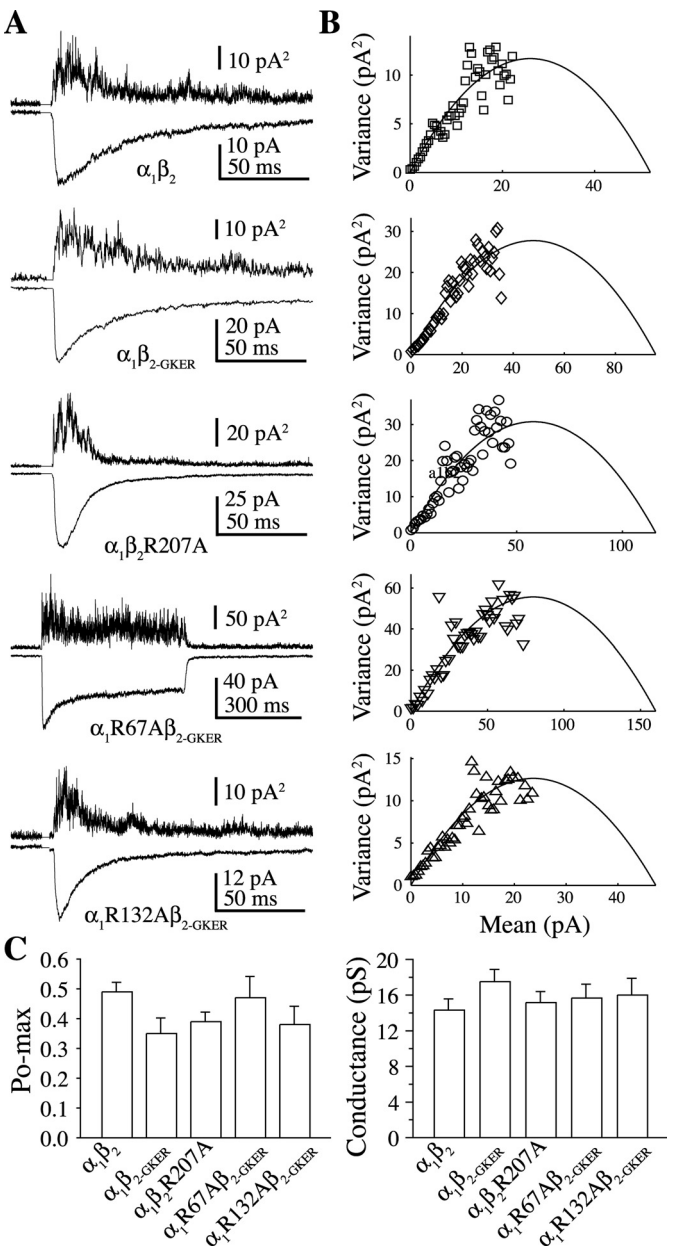

Fig. 6. None of the mutants altered the peak open probability ($P_{o\text{-}max}$) of the channel. A, mean (below) and variance (above) of consecutive responses to 2 or 500 ms pulses of 10 mM GABA. B, plots of normalized mean current versus variance for the traces shown in A fit with a parabola (black line) describing the single-channel conductance, $P_{o\text{-}max}$, and the number of channels present in each patch (Sigworth, 1980). C, summary of $P_{o\text{-}max}$ and single-channel conductance from the fits in B. No differences were found by one-way ANOVA with post hoc Tukey's test, $p < 0.05$.

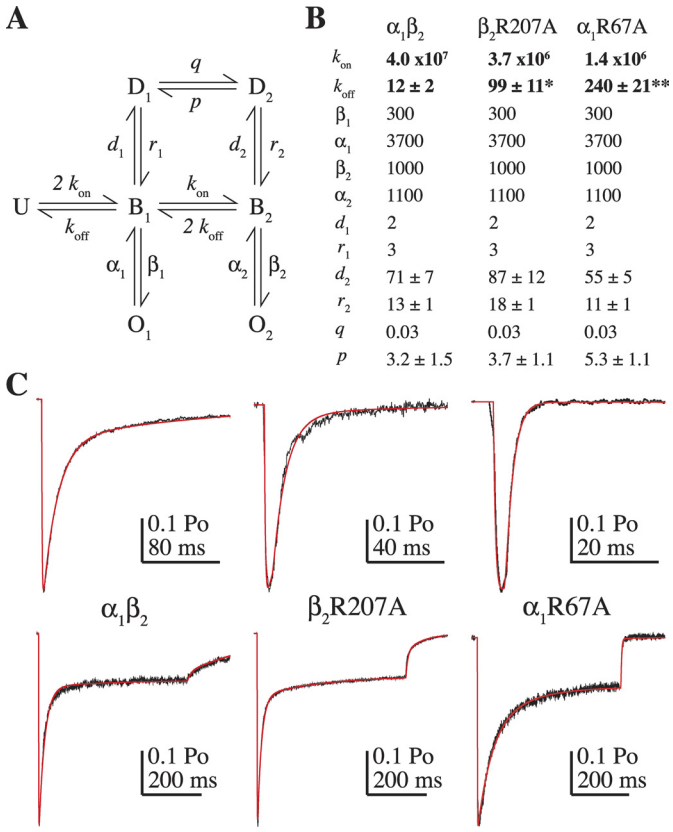

	$\alpha_1\beta_2$	β_2R207A	α_1R67A
k_{on}	**4.0 x10⁷**	**3.7 x10⁶**	**1.4 x10⁶**
k_{off}	**12 ± 2**	**99 ± 11***	**240 ± 21****
β_1	300	300	300
α_1	3700	3700	3700
β_2	1000	1000	1000
α_2	1100	1100	1100
d_1	2	2	2
r_1	3	3	3
d_2	71 ± 7	87 ± 12	55 ± 5
r_2	13 ± 1	18 ± 1	11 ± 1
q	0.03	0.03	0.03
p	3.2 ± 1.5	3.7 ± 1.1	5.3 ± 1.1

Fig. 7. Kinetic modeling demonstrates that the kinetic effects of the mutations β_2R207A and α_1R67A can be explained by slower GABA binding and faster unbinding. A, the Markov model used to simulate GABA-evoked currents (U, unbound; B, bound; O, open; D, desensitized; previously described in Jones et al., 1998). B, rate constants used to simulate $\alpha_1\beta_2$, R207A, and R67A receptors (units are in seconds^{-1} except for GABA binding steps k_{on} and q, which are $M^{-1} \cdot s^{-1}$). The values of k_{off}, d_2, r_2, and p are reported as mean ± S.E.M. because they were allowed to vary. The model was optimized to fit current responses to 2 to 4 ms and 500-ms pulses of 10 to 30 mM GABA from individual patches (see *Materials and Methods*). k_{off} was the only unconstrained rate constant that significantly differed comparing mutant and wild-type models (one-way ANOVA with post hoc Tukey's test, *, $p < 0.05$, **, $p < 0.01$). C, current responses (black) evoked by 2 to 4 ms (top) and 500-ms (bottom) pulses of 10 to 30 mM GABA from individual patches containing $\alpha_1\beta_2$ (left), $\alpha_1\beta_2$R207A (middle) and α_1R67A$\beta_{2\text{-GKER}}$ (right) receptors overlaid with simulated responses (red). Note the different time scales for the short pulses.

of the receptor (Fig. 6). Because $P_{o\text{-}max}$ is a measure that depends on the interplay between numerous microscopic transitions, it is useful not only as a general measure of microscopic kinetic changes but also as a constraint on any kinetic model of the receptor (see below). None of the mutations altered either conductance (γ) at −60 mV or $P_{o\text{-}max}$ ($\alpha_1\beta_2$: $\gamma = 14.3 \pm 1.2$ pS, $P_{o\text{-}max} = 0.49 \pm 0.03$, $n = 10$; $\alpha_1\beta_{2\text{-GKER}}$: $\gamma = 17.5 \pm 1.3$ pS, $P_{o\text{-}max} = 0.35 \pm 0.05$, $n = 5$; α_1R67A$\beta_{2\text{-GKER}}$: $\gamma = 15.7 \pm 1.2$ pS, $P_{o\text{-}max} = 0.47 \pm 0.07$, $n = 19$; α_1R132A$\beta_{2\text{-GKER}}$: $\gamma = 16 \pm 1.8$ pS, $P_{o\text{-}max} = 0.38 \pm 0.06$, $n = 3$; $\alpha_1\beta_2$R207A: $\gamma = 15.2 \pm 1.2$ pS, $P_{o\text{-}max} = 0.39 \pm 0.03$; $n = 17$). The larger single-channel conductances obtained from nonstationary variance analysis than those measured directly in the single-channel recordings above is probably due to the fact that the former reflects a weighted average of all conductance levels, whereas the latter only measures openings to the most frequent level. We were not able to quantitatively confirm this, however, because subconductances did not appear as distinct peaks in all-points amplitude histograms. These data suggest that α_1Arg67 and β_2Arg207 are not involved in channel gating, whereas α_1Arg132 has an effect on the stability of the open channel.

The Kinetic Effects of α_1R67A and β_2R207A Are Due to Slower GABA Binding and Faster Unbinding. Given that those mutations having the largest effects on the microscopic GABA binding rate also had the largest effects on macroscopic deactivation, and also that binding and unbinding rates are often inversely correlated (Jones et al., 1998, 2001; Mozrzymas et al., 1999; Barberis et al., 2000), we hypothesized that the macroscopic effects of the mutations on

deactivation were entirely due to faster GABA unbinding. Unlike the binding rate, we could not examine this directly, but instead we asked whether such a hypothesis could explain our observations using a kinetic model shown previously to account for multiple aspects of $GABA_A$ receptor behavior (Fig. 7A) (Jones et al., 1998; Wagner et al., 2004; Goldschen-Ohm et al., 2010).

The model shown in Fig. 7A was optimized for individual patches by fitting current responses to 2 to 4 ms and 500-ms pulses of 10 to 30 mM GABA for $\alpha_1\beta_2$ (7 patches), $\alpha_1\beta_2$R207A (7 patches), and α_1R67A$\beta_{2\text{-GKER}}$ (10 patches) receptors (Fig. 7C, see *Materials and Methods*). We were able to quantitatively replicate all observed macroscopic effects of β_2R207A and α_1R67A on responses to brief and long GABA pulses by 1) decreasing the GABA binding rate as measured above (see Table 2), and 2) increasing the GABA unbinding rate. The final rate constants (mean ± S.E.M.) are listed in Fig. 7B. Thus, the model illustrated in Fig. 7 is consistent with the idea that α_1Arg67 and β_2Arg207 are involved in GABA binding and unbinding and have little or no effect on channel gating.

Discussion

Despite the wealth of information gained from mutagenesis, functional assays, and crystallography of homologous proteins (Sigel et al., 1992; Amin and Weiss, 1993; Smith and Olsen, 1994; Boileau et al., 1999, 2002; Westh-Hansen et al., 1999; Brejc et al., 2001; Wagner and Czajkowski, 2001; Cromer et al., 2002; Holden and Czajkowski, 2002; Newell and Czajkowski, 2003; Celie et al., 2004; Wagner et al., 2004; Hansen et al., 2005; O'Mara et al., 2005), the exact structure of the GABA binding site and the roles of individual residues in ligand binding and the accompanying conformational changes remain unclear. Most previous studies of the binding site have relied on changes in dose-response curve macroscopic measures (e.g., EC_{50}) that are influenced by both binding and gating and thus cannot separate them (Colquhoun, 1998). We therefore used kinetic methods to separate the roles in binding versus gating of three arginines lining the GABA-binding intersubunit interface of the human $GABA_A$ receptor (α_1Arg67, α_1Arg132, and β_2Arg207). Individual alanine mutations lowered affinity for GABA and accelerated deactivation with little or no effect on desensitization. A combination of macroscopic and single-channel measurements with kinetic modeling demonstrated that for the mutations α_1R67A and β_2R207A, these effects can be entirely explained by a 10- to 14-fold slower microscopic GABA binding rate and 8- to 20-fold faster unbinding rate. Therefore, these two residues contribute to both the rapid formation and stability of the agonist-bound complex, with little or no involvement in channel gating. A parsimonious interpretation is that one or both of these arginines interacts directly with the carboxylate group of the GABA molecule, although it is also possible that they contribute structurally to the integrity of the binding site.

Unlike the other two mutations, α_1R132A did not affect the GABA binding rate. Given that α_1R132A$\beta_{2\text{-GKER}}$ deactivates more quickly than wild type, this seems to suggest that α_1Arg132 influences only GABA unbinding but not binding. However, because agonist binding and unbinding rates are typically inversely correlated (Jones et al., 1998, 2001; Mozrzymas et al., 1999; Barberis et al., 2000), the modest speeding of deactivation by α_1R132A suggests that a slowing of GABA binding may be present but too small to detect with our methods. Interestingly, single-channel recordings from α_1R132A$\beta_{2\text{-GKER}}$ receptors exhibited a small number of openings to a new long-lived open state. Although these long openings comprised only ~1% of all openings, they account for ~11% of the observed charge. These long openings could prolong deactivation, potentially masking some of the effects of faster ligand unbinding.

Two mutations (β_2R207A and α_1R132A) reduced SR-95531 affinity by speeding its unbinding rate 2- to 9-fold without altering its binding rate, indicating that these arginines maintain the stability of the antagonist-receptor complex but do not influence its formation. In contrast, α_1R67A increased antagonist affinity by speeding binding 5-fold without changing unbinding, indicating that this arginine hinders formation of the antagonist-receptor complex but does not influence its stability once formed. Therefore, α_1Arg67 is part of the energy barrier to formation of the antagonist-receptor complex, whereas β_2Arg207 and α_1Arg132 are part of the energy well that stabilizes this complex. The SR-95531 molecule may thus encounter steric or electrostatic resistance to entering the pocket from α_1Arg67 but once in the pocket may interact directly with β_2Arg207 and α_1Arg132 to form the antagonist-bound state. Alternatively, β_2Arg207 and α_1Arg132 could contribute structurally to the stability of the antagonist binding site.

Antagonism upon Binding of a Single Molecule of SR-95531. Despite the presence of two agonist sites, the monoexponential unbinding time courses of several antagonists suggest that antagonism is relieved upon unbinding from a single site (Jones et al., 1998, 2001; Wagner et al., 2004). In addition, antagonist Hill slopes near unity suggest that antagonism occurs upon binding to only a single site. One explanation for these results is that SR-95531 binds to only one of the two GABA binding sites. However, a study of receptors formed from concatenated subunits containing mutations in none, both, or one or the other GABA binding site suggest that both sites have a similar affinity for the competitive antagonists SR-95531 and bicuculline (Baumann et al., 2003). This suggests that SR-95531 can bind at either site, but allosterically inhibits its binding to the other site. Indeed, competitive antagonists can exert allosteric effects on channel activation (Ueno et al., 1997), and can alter the accessibility of residues at both of the β/α GABA binding interfaces (Boileau et al., 2002) and the α/γ benzodiazepine binding interface (Sharkey and Czajkowski, 2008). Interestingly, competitive antagonists for the homologous nACh receptor known to bind preferentially to one or the other nonidentical binding site illustrate that binding of a single antagonist molecule is sufficient to prevent channel opening in a cysteine-loop receptor (Wenningmann and Dilger, 2001; Dilger et al., 2007). Furthermore, pairs of nACh receptor antagonists often exhibit cooperative effects, possibly because antagonist binding at one site allosterically influenced antagonist binding at the other site (Liu and Dilger, 2008). We conclude that SR-95531 either preferentially binds to only one of the two GABA binding sites or allosterically inhibits itself from binding to both sites simultaneously.

Arginines Are Similarly Involved in GABA and THIP Binding. Interestingly, the two mutations having the larg-

est effect on the GABA binding rate (α_1R67A and β_2R207A) had similar effects on the binding rate of the lower affinity agonist THIP, suggesting that those arginines may be part of a generic mechanism underlying agonist binding. Consistent with the idea that α_1Arg67 is generally involved in agonist binding, molecular dynamics simulations with GABA and glycine docked to homology models of the $GABA_C$ and glycine receptors, respectively, show the carboxylate group of both ligands in direct contact with the amide head group of an arginine in a homologous position to α_1Arg67 in the $GABA_A$ receptor (Grudzinska et al., 2005; Melis et al., 2008). A glutamate-gated chloride channel having 34% sequence identity to the human α1 glycine receptor has been crystallized with glutamate bound in the agonist binding site, in which its carboxylate groups are coordinated by two arginines, one of which is located similarly to α_1Arg67 in the $GABA_A$ receptor (Hibbs and Gouaux, 2011).

Aromatic Residues in the Binding Site. A number of highly conserved aromatic residues form the so-called "aromatic box" and have been widely implicated in GABA binding as a result of the large reduction in GABA affinity seen upon their mutation (Sigel et al., 1992; Amin and Weiss, 1993; Boileau et al., 1999, 2002; Wagner and Czajkowski, 2001). In particular, unnatural amino acid substitution showed that the apparent affinity for GABA in the $GABA_A$ and $GABA_C$ receptors correlates with the electronegativity of the π-electron orbitals of β_2Tyr97 and ρ_1Tyr198, respectively, suggesting that the GABA amine group may form cation-π bonds with these residues (Lummis, 2009). Given that these aromatics are on opposite sides of the interface, this requires that the orientation of GABA in the pocket is different for these two receptors. An alternative but so far unexplored possibility is that the correlation of aromatic electronegativity with apparent affinity reflects not the formation of cation-π bonds with the agonist but rather with the amide head group of a nearby arginine that stabilizes binding pocket structure. Interestingly, arginines involved in cation-π interactions with aromatics retain their hydrogen bonding capability. A survey of crystal structures found that whenever an arginine/aromatic pair interacted with a ligand, hydrogen bonding to the arginine was always involved, and direct contacts between the ligand and the aromatic were often seen as well (Flocco and Mowbray, 1994). Thus, aromatics may play an important role in the positioning of arginines for proper interaction with ligands.

Conclusions

We conclude that α_1Arg67 and β_2Arg207 participate primarily in agonist binding and unbinding, but not gating of the channel, and are thus good candidates to interact directly with the GABA and THIP molecules. Given that these two residues are on opposite sides of the β/α binding interface, it remains unclear whether they might simultaneously interact with the bound ligand or rather sequentially interact as part of a binding/unbinding pathway involving multiple steps or may simply contribute to the stability of the binding site. In addition, α_1Arg67 poses a barrier to binding of the competitive antagonist SR-95531, whereas α_1Arg132 and β_2Arg207 stabilize the bound antagonist. In addition, α_1Arg132 does influence the stability of the open channel and thus may participate in transducing binding to opening of the channel gate.

The microscopic binding and unbinding rates reported here are directly related to the energy landscape seen by these ligands during binding and unbinding and thus represent an important set of experimental constraints for validating atomic level models of the GABA binding site and future molecular dynamics simulations. Knowledge of the separate roles of residues in binding versus gating will be invaluable in improving our understanding of how ligand binding alters the receptor structure to cause channel activation.

Authorship Contributions

Participated in research design: Goldschen-Ohm, Wagner, and Jones.

Conducted experiments: Goldschen-Ohm and Wagner.

Performed data analysis: Goldschen-Ohm and Wagner.

Wrote or contributed to the writing of the manuscript: Goldschen-Ohm, Wagner, and Jones.

References

Amin J and Weiss DS (1993) $GABA_A$ receptor needs two homologous domains of the β-subunit for activation by GABA but not by pentobarbital. *Nature* **366:**565–569.

Barberis A, Cherubini E, and Mozrzymas JW (2000) Zinc inhibits miniature GABAergic currents by allosteric modulation of $GABA_A$ receptor gating. *J Neurosci* **20:**8618–8627.

Baumann SW, Baur R, and Sigel E (2003) Individual properties of the two functional agonist sites in GAB_A receptors. *J Neurosci* **23:**11158–11166.

Boileau AJ, Evers AR, Davis AF, and Czajkowski C (1999) Mapping the agonist binding site of the $GABA_A$ receptor: evidence for a β-strand. *J Neurosci* **19:**4847–4854.

Boileau AJ, Newell JG, and Czajkowski C (2002) $GABA_A$ receptor β_2 Tyr^{97} and Leu^{99} line the GABA-binding site. Insights into mechanisms of agonist and antagonist actions. *J Biol Chem* **277:**2931–2937.

Bollan K, King D, Robertson LA, Brown K, Taylor PM, Moss SJ, and Connolly CN (2003) $GABA_A$ receptor composition is determined by distinct assembly signals within α and β subunits. *J Biol Chem* **278:**4747–4755.

Brejc K, van Dijk WJ, Klaassen RV, Schuurmans M, van Der Oost J, Smit AB, and Sixma TK (2001) Crystal structure of an ACh-binding protein reveals the ligand-binding domain of nicotinic receptors. *Nature* **411:**269–276.

Celie PH, van Rossum-Fikkert SE, van Dijk WJ, Brejc K, Smit AB, and Sixma TK (2004) Nicotine and carbamylcholine binding to nicotinic acetylcholine receptors as studied in AChBP crystal structures. *Neuron* **41:**907–914.

Clements JD, Lester RA, Tong G, Jahr CE, and Westbrook GL (1992) The time course of glutamate in the synaptic cleft. *Science* **258:**1498–1501.

Colquhoun D (1998) Binding, gating, affinity and efficacy: the interpretation of structure-activity relationships for agonists and of the effects of mutating receptors. *Br J Pharmacol* **125:**924–947.

Colquhoun D and Hawkes AG (1995) A Q-matrix cookbook. How to write only one program to calculate the single-channel and macroscopic predictions for any kinetic mechanism, in *Single-Channel Recording*, 2nd ed (Sakmann B and Neher E, eds) pp 589–633, New York, Plenum.

Colquhoun D and Sigworth FJ (1995) Fitting and statistical analysis of single-channel records, in *Single-Channel Recording*, 2nd ed (Sakmann B and Neher E, eds) pp 483–587, New York, Plenum.

Cromer BA, Morton CJ, and Parker MW (2002) Anxiety over $GABA_A$ receptor structure relieved by AChBP. *Trends Biochem Sci* **27:**280–287.

Dilger JP, Vidal AM, Liu M, Mettewie C, Suzuki T, Pham A, and Demazumder D (2007) Roles of amino acids and subunits in determining the inhibition of nicotinic acetylcholine receptors by competitive antagonists. *Anesthesiology* **106:**1186–1195.

Flocco MM and Mowbray SL (1994) Planar stacking interactions of arginine and aromatic side-chains in proteins. *J Mol Biol* **235:**709–717.

Goldschen-Ohm MP, Wagner DA, Petrou S, and Jones MV (2010) An epilepsy-related region in the $GABA_A$ receptor mediates long-distance effects on GABA and benzodiazepine binding sites. *Mol Pharmacol* **77:**35–45.

Grudzinska J, Schemm R, Haeger S, Nicke A, Schmalzing G, Betz H, and Laube B (2005) The β subunit determines the ligand binding properties of synaptic glycine receptors. *Neuron* **45:**727–739.

Hansen SB, Sulzenbacher G, Huxford T, Marchot P, Taylor P, and Bourne Y (2005) Structures of *Aplysia* AChBP complexes with nicotinic agonists and antagonists reveal distinctive binding interfaces and conformations. *EMBO J* **24:**3635–3646.

Hibbs RE and Gouaux E (2011) Principles of activation and permeation in an anion-selective Cys-loop receptor. *Nature* **474:**54–60.

Holden JH and Czajkowski C (2002) Different residues in the $GABA_A$ receptor α_1T60-α_1K70 region mediate GABA and SR-95531 actions. *J Biol Chem* **277:**18785–18792.

Jones MV, Jonas P, Sahara Y, and Westbrook GL (2001) Microscopic kinetics and energetics distinguish $GABA_A$ receptor agonists from antagonists. *Biophys J* **81:**2660–2670.

Jones MV, Sahara Y, Dzubay JA, and Westbrook GL (1998) Defining affinity with the $GABA_A$ receptor. *J Neurosci* **18:**8590–8604.
Jordan M, Schallhorn A, and Wurm FM (1996) Transfecting mammalian cells: optimization of critical parameters affecting calcium-phosphate precipitate formation. *Nucleic Acids Res* **24:**596–601.
Kucken AM, Wagner DA, Ward PR, Teissére JA, Boileau AJ, and Czajkowski C (2000) Identification of benzodiazepine binding site residues in the γ2 subunit of the γ-aminobutyric $acid_A$ receptor. *Mol Pharmacol* **57:**932–939.
Liu M and Dilger JP (2008) Synergy between pairs of competitive antagonists at adult human muscle acetylcholine receptors. *Anesth Analg* **107:**525–533.
Lummis SC (2009) Locating GABA in GABA receptor binding sites. *Biochem Soc Trans* **37:**1343–1346.
Melis C, Lummis SC, and Molteni C (2008) Molecular dynamics simulations of GABA binding to the $GABA_C$ receptor: the role of Arg104. *Biophys J* **95:**4115–4123.
Mozrzymas JW, Barberis A, Michalak K, and Cherubini E (1999) Chlorpromazine inhibits miniature GABAergic currents by reducing the binding and by increasing the unbinding rate of $GABA_A$ receptors. *J Neurosci* **19:**2474–2488.
Newell JG and Czajkowski C (2003) The $GABA_A$ receptor α_1 subunit Pro^{174}-Asp^{191} segment is involved in GABA binding and channel gating. *J Biol Chem* **278:**13166–13172.
O'Mara M, Cromer B, Parker M, and Chung SH (2005) Homology model of the $GABA_A$ receptor examined using Brownian dynamics. *Biophys J* **88:**3286–3299.
Sharkey LM and Czajkowski C (2008) Individually monitoring ligand-induced changes in the structure of the $GABA_A$ receptor at benzodiazepine binding site and non-binding site interfaces. *Mol Pharmacol* **74:**203–212.
Sigel E, Baur R, Kellenberger S, and Malherbe P (1992) Point mutations affecting antagonist affinity and agonist dependent gating of $GABA_A$ receptor channels. *EMBO J* **11:**2017–2023.
Sigworth FJ (1980) The variance of sodium current fluctuations at the node of Ranvier. *J Physiol* **307:**97–129.
Smith GB and Olsen RW (1994) Identification of a [^{3}H]muscimol photoaffinity substrate in the bovine γ-aminobutyric $acid_A$ receptor a subunit. *J Biol Chem* **269:**20380–20387.
Taylor PM, Thomas P, Gorrie GH, Connolly CN, Smart TG, and Moss SJ (1999) Identification of amino acid residues within $GABA_A$ receptor β subunits that mediate both homomeric and heteromeric receptor expression. *J Neurosci* **19:**6360–6371.
Ueno S, Bracamontes J, Zorumski C, Weiss DS, and Steinbach JH (1997) Bicuculline and gabazine are allosteric inhibitors of channel opening of the $GABA_A$ receptor. *J Neurosci* **17:**625–634.
Wagner DA and Czajkowski C (2001) Structure and dynamics of the GABA binding pocket: A narrowing cleft that constricts during activation. *J Neurosci* **21:**67–74.
Wagner DA, Czajkowski C, and Jones MV (2004) An arginine involved in GABA binding and unbinding but not gating of the $GABA_A$ receptor. *J Neurosci* **24:**2733–2741.
Wenningmann I and Dilger JP (2001) The kinetics of inhibition of nicotinic acetylcholine receptors by (+)-tubocurarine and pancuronium. *Mol Pharmacol* **60:**790–796.
Westh-Hansen SE, Witt MR, Dekermendjian K, Liljefors T, Rasmussen PB, and Nielsen M (1999) Arginine residue 120 of the human $GABA_A$ receptor α_1 subunit is essential for GABA binding and chloride ion current gating. *Neuroreport* **10:**2417–2421.

Address correspondence to: Dr. Marcel P. Goldschen-Ohm, Department of Physiology, University of Wisconsin-Madison, Madison, WI 53706. E-mail: marcel.goldschen@gmail.com